

Mesopic and Dark-Adapted Two-Color Fundus-Controlled Perimetry in Choroidal Neovascularization Secondary to Age-Related Macular Degeneration

Leon von der Emde¹, Maximilian Pfau^{1,2}, Sarah Thiele^{1,2}, Philipp T. Möller^{1,2}, Ruth Hassenrik¹, Monika Fleckenstein^{1,2}, Frank G. Holz^{1,2}, and Steffen Schmitz-Valckenberg^{1,2}

¹ Department of Ophthalmology, University of Bonn, Ernst-Abbe-Str. 2, Bonn, Germany

² GRADE Reading Center, University of Bonn, Ernst-Abbe-Str. 2, Bonn, Germany

Correspondence: Steffen Schmitz-Valckenberg, Department of Ophthalmology, University of Bonn, Ernst-Abbe-Str. 2, 53127 Bonn, Germany. e-mail: steffen.schmitz-valckenberg@ukbbonn.de

Received: 23 August 2018

Accepted: 17 October 2018

Published: 9 January 2019

Keywords: retest reliability; two-color FCP; patient reliability indices; microperimetry

Citation: von der Emde L, Pfau M, Thiele S, Möller PT, Hassenrik R, Fleckenstein M, Holz FG, Schmitz-Valckenberg S. Mesopic and dark-adapted two-color fundus-controlled perimetry in choroidal neovascularization secondary to age-related macular degeneration. *Trans Vis Sci Tech.* 2019;8(1):7, <https://doi.org/10.1167/tvst.8.1.7>
Copyright 2019 The Authors

Purpose: To determine the retest variability of mesopic and two-color dark-adapted (DA) fundus-controlled perimetry (FCP), to evaluate the predictive value of patient reliability indices, and to analyze the extent of impairment of rod- and cone function in neovascular age-related macular degeneration (nAMD).

Methods: A total of 50 eyes of 50 patients with nAMD (mean age, 76.1 years) and 70 eyes of 70 age-similar normal subjects underwent multimodal imaging as well as mesopic and DA two-color perimetry using the S-MAIA device. A subset of patients ($n = 28$) underwent duplicate testing for retest reliability assessment. Mixed models were used for analysis of the hierarchical data.

Results: In eyes with nAMD, the coefficient of repeatability was (mean \pm standard deviation [SD]) 5.99 ± 1.55 dB for mesopic, 6.14 ± 2.19 dB for DA cyan, and 6.06 ± 1.09 dB for DA red testing. “Patient reliability indices” explained 55%, 54.2%, and 64.2% of the variance in retest variability. The mean sensitivity loss was greater for DA cyan compared to DA red testing (cyan-red differences [mean \pm SD] -2.63 ± 3.87 dB, $P < 0.001$).

Conclusions: The relatively greater degree of DA cyan versus DA red sensitivity loss indicates preferential rod vulnerability in nAMD, and qualifies rod function-based outcomes measures as potential sensitive and early markers of treatment response in nAMD.

Translational Relevance: The S-MAIA allows reliable testing of mesopic, DA cyan, and DA red sensitivity in patients with nAMD. Patient reliability indices may serve as eligibility criteria for clinical trials to identify patients with adequate retest reliability.

Introduction

Age related macular degeneration (AMD) is among the leading causes of severe visual impairment in developed countries.¹ In recent years, introduction of anti-vascular endothelial growth factor (anti-VEGF) therapy has significantly improved visual outcomes in patients with choroidal neovascularizations (CNV), the exudative late-stage manifestation (nAMD).^{2,3} However, while anti-VEGF monotherapy can achieve excellent visual outcomes over 12 to 24 months, the

long-term outcomes are less favorable with loss of best-corrected visual acuity (BCVA) of 15 letters or more in a third of patients.⁴ Until now, innovative approaches; that is, combination therapies targeting VEGF and platelet-derived growth factor (PDGF) signaling, have not yet definitely demonstrated any additional benefit (e.g., CAPELLA, [clinicaltrials.gov identifier: NCT02418754], OPH1002 [NCT01944839], OPH1003 [NCT01940900]).

While no significant improvement in function could be attributable to a lack of therapeutic effectiveness, it may be argued that the utility of

BCVA as a functional endpoint is limited. Of note, BCVA primarily tests cone function at the fovea (or the preferred retinal locus in eyes with extrafoveal fixation). Therefore, some degree of foveal involvement was a common inclusion criterion in Phase III trials for anti-VEGF therapy, excluding systematically early extrafoveal or peripapillary CNV.^{5–7} In addition, BCVA exhibits a significant ceiling effect that may prohibit the recognition of treatment effects in eyes with good pretreatment BCVA, resulting in clinical trial designs that exclude early lesions with good visual acuity.⁸ Overall, it would be desirable to overcome the limitations of BCVA particularly in nAMD by establishing additional and more sensitive functional endpoints.

As a potential alternative, fundus-controlled perimetry (FCP, also termed microperimetry) allows for spatially resolved testing of retinal sensitivity over the entire macula area, even in patients with unstable fixation. In intermediate AMD, FCP has allowed to detect subtle changes in visual function even in patients with good BCVA.^{9,10} In nAMD, mesopic FCP proved useful to assess retinal sensitivity in relation to specific lesion components and allowed for quantification of treatment effects.^{11,12} FCP allowed for detection of progressive loss of retinal sensitivity even in patients with no disease activity, stable BCVA, and unchanged central retinal thickness.¹³ However, we are aware of only one study conducted to date that examined the reproducibility of FCP testing in CNV secondary to AMD.¹⁴ Furthermore, no data with regard to dark-adapted FCP in exudative AMD are available. Yet, rod dysfunction was shown to exceed cone dysfunction in many macular diseases, including nonneovascular AMD stages.^{15–17} Recently, the refined and selective probing of rod function by two-color dark-adapted (DA) FCP has become possible with the introduction of the S-MAIA (Centervue, Padua, Italy) device.^{17–20}

For FCP testing to be applicable in clinical trials, it is mandatory to be able to identify patients with a good retest reliability. “Patient-reliability indices,” such as suprathreshold stimuli presentation to the optic nerve head (i.e., false-positive catch trials [Heijl-Krakau method]), may help to select such suitable patients.²¹ However, to date, the predictive value of these “patient-reliability indices” with regard to the retest reliability in the setting of FCP is unknown. This includes the predictive value of global factors affecting all test-points in a given patient (e.g., age, fixation stability, false-positive response rate) and

local factors affecting the retest reliability of a given test point (e.g., location-specific sensitivity).

We determined the retest variability of mesopic and dark-adapted two-color FCP in CNV secondary to AMD to define the clinical significance of change over time as prerequisite for clinical trials. Further, we investigated the predictive value of “patient-reliability indices” for forecasting retest reliability of patients, such as false-positive responses, which may serve as eligibility/exclusion criteria for clinical trials. Finally, we described the degree of functional loss for the CNV subgroups in relation to the dynamic range of the device and of BCVA testing.

Methods

Subjects

Subjects with nAMD were recruited from clinics of the Department of Ophthalmology, University of Bonn, Germany. Inclusion criteria were at least 50 years of age, a CNV lesion seen in optical coherence tomography angiography (OCT-A), fluorescein angiography, and/or indocyanine green angiography (ICG-A) and no prior intraocular surgery of the eye with the exception of cataract surgery. Exclusion criteria included refractive errors ≥ 5.00 diopters of spherical equivalent and >1.50 diopters of astigmatism assessed by autorefractometry (ARK-560A; Nidek, Gamagori, Japan), as well as a history of glaucoma or relevant anterior segment diseases with media opacities. If both eyes met the inclusion criteria, the eye with better BCVA was included. Apart from taking the medical history, all subjects underwent routine ophthalmologic examinations, including BCVA, slit-lamp, and funduscopic examination. Control eyes were recruited from the hospital wards among patients with a healthy fellow eye and patient’s companions. The institutional review board of the University of Bonn approved the study (ethics approval ID: 191/16). Written informed consent conforming to the tenets of the Declaration of Helsinki was acquired from all participants.

Imaging Protocol

Standardized retinal imaging was performed including combined confocal laser ophthalmoscopy (cSLO) and spectral-domain optical coherence tomography (SD-OCT) imaging ($30^\circ \times 25^\circ$, ART 25, 121 B-scans, Spectralis HRA-OCT 2; Heidelberg Engineering, Heidelberg, Germany). Furthermore, 30° fundus autofluorescence (FAF) and multicolor

imaging as well as 55° FAF imaging were performed on the same device. OCT-A was performed using a swept-Source OCT (SS-OCT) device (3 × 3 mm, 6 × 6 mm, 9 × 9 mm OCT-A scan, PLEX Elite 9000; Carl Zeiss Meditec AG, Jena, Germany). Last, color fundus photography (CFP) was performed (Visucam 500, Carl Zeiss Meditec AG).

Classification of CNV Activity

Within the spectrum of nAMD, CNV subtypes may be differentiated according to the disease activity. Active CNV (aCNV) was defined by evidence of exudation (intra- or subretinal fluid, retinal hemorrhages) requiring treatment every 4 to 12 weeks, while other patients classified as silent CNV (sCNV) herein exhibit no signs of exudation even if therapy is halted for periods longer than 12 weeks. Finally, treatment-naïve “quiescent” CNV (qCNV), as described by Querques et al.²² is recognized by the absence of any current (or former) signs of exudation and was primarily determined by OCT-A imaging.^{22–24}

Fundus-Controlled Perimetry

FCP testing was done after dilating pupils using 2.5% phenylephrine and 0.5% tropicamide to facilitate fundus tracking. Patients with no prior perimetry experience underwent a short mesopic practice FCP test to accustom them to the procedure. Patients underwent duplicate (28 of 50 patients) or singular (22 of 50 patients) mesopic (achromatic stimuli, 400–800 nm) FCP, with subsequent 30 minutes of dark adaptation (light level < 0.1 lux), followed by duplicate or singular dark-adapted cyan (505 nm) and finally dark-adapted red (627 nm) FCP using the S-MAIA device. Testing was performed with the preset 4-2 dB staircase strategy. The stimulus size was 0.43° (Goldmann III). The test grid consisted of 61 stimuli covering the central 18° of the retina. The test points were evenly distributed in five rings at 1°, 3°, 5°, and 9° around a central test point.

False-positive responses were measured through presentation of suprathreshold stimuli to the optic nerve head (i.e., Heijl-Krakau method). Furthermore, the rate of wrong pressure events was measured as the number of pressure events outside of the response window of the S-MAIA divided by the examination time.²¹ Last, the 95% bivariate contour ellipse area (BCEA) encompassing 95% of the fixation points was recorded as measure of fixation stability.²⁵

Statistical Analysis

Statistical analyses were performed using the software environment R. The visual acuity was converted to the logarithm of the Minimum Angle of Resolution (logMAR). Mixed model analysis was used to consider the hierarchical dependencies of the data (test points nested in eye). *P* values were obtained through likelihood ratio tests. The normative data were age-adjusted (to match an age of 76 years) through linear regression on the level of each test point as previously described.¹⁷ The mean sensitivity was calculated as the mean value for each patient. The pointwise sensitivity loss and mean sensitivity loss represented the deviation from the respective normal values. The Bland–Altman diagrams and coefficients of repeatability (CoR) were plotted/calculated as specified by Bland and Altman.²⁶ The coefficient-of-determination (R^2) was used to assess the between-subject variance in retest variability explained by “patient reliability indices” through multiple linear regression with averaging over orderings of regressors. Please note, the control group was only used to calculate the pointwise sensitivity loss and mean sensitivity loss and excluded for all other analyses (i.e., analysis of retest reliability and analysis of the retest variability explained by “patient reliability indices”).

Results

Demographics

A total of 50 eyes of 50 patients with CNV secondary to AMD (mean age ± SD, 76.1 ± 7.6 years; range, 54.6–90.2 years) and 70 eyes of 70 controls (55.9 ± 17.9 years; range 21.8–84.5 years) were included in the study (Table 1). The normative data were age-adjusted through regression analysis (cf. Methods). The median BCVA was logMAR 0.38 (Snellen equivalent approximately 20/50) ± 0.34 for patients. Active CNV (i.e., patients requiring treatment every 4 to 12 weeks) was present in 32 patients (BCVA of logMAR 0.41 [20/50] ± 0.35). Eleven patients exhibited sCNV (BCVA of logMAR 0.49 [20/63] ± 0.35) and seven exhibited treatment-naïve qCNV (logMAR 0.08 [20/25] ± 0.07).

Retest Reliability

A total of 28 patients were randomly selected for duplicate testing to determine the retest reliability (age 76.5 ± 7.3 years). In terms of age, BCVA, and CNV

Table 1. Cohort Characteristics

Characteristic	CNV Patients, N = 50	Retest Subgroup of CNV Patients, N = 28	Normal Subjects, N = 70
Age, mean ± SD	76.1 ± 7.6 years	76.5 ± 7.3 years	55.9 ± 16.9 years
Sex	30 female 20 male	18 female 10 male	23 female 47 male
BCVA, mean ± SD	0.38 ± 0.34 logMAR	0.38 ± 0.33 logMAR	0.03 ± 0.05
CNV subtype	32 active CNV 11 silent CNV 7 quiescent CNV	18 active CNV 6 silent CNV 4 quiescent CNV	NA

The cohort characteristics are outlined. The randomly sampled subgroup of patients that underwent duplicate testing is highly representative of the overall cohort. Please note that the normal subjects were not included for the analysis of retest reliability or the analysis of the “patient reliability indices.” The perimetry data of the normal subjects were age-adjusted as previously described in detail and solely used to determine the point-wise sensitivity loss.

lesion subtypes, this subset was representative of the overall cohort (Table 1). An overview of the examination time, fixation stability and “patient reliability indices” is shown in Table 2. The CoR – the range within which 95% of test–retest measurement differences lie – was (mean ± SD) 5.99 ± 1.55 dB for mesopic, 6.14 ± 2.19 dB for dark-adapted cyan, and 6.06 ± 1.79 dB for dark-adapted red testing. These differences in CoR among the three examined test types were not significant (repeated measures ANOVA, *P* = 0.753). The cyan-red difference had a CoR of 8.52 ± 2.09 dB. Accordingly, the cumulative percentage of test points with retest differences of ±2

dB or less was 73.9% for mesopic, 79.2% for DA cyan, and 75.1% for DA red testing, respectively (Table 3). Bland-Altman plots for all three types of testing exhibited convergence of the measurements towards the lower end of the dynamic range indicating that a significant proportion of measurements fell within the minimum value (Fig. 2). This floor effect was especially pronounced for dark-adapted cyan testing. In contrast, for all three types of testing, no ceiling effect was observed (Fig. 2). For the mean sensitivity, the 95% CoR was 1.31 ± 1.12 dB for mesopic, 1.19 ± 0.95 dB for dark-adapted cyan, and 0.89 ± 0.72 dB for dark-adapted red testing.

Table 2. Examination Time, Fixation Stability and Patient Reliability Indices

Characteristic	Overall Cohort (N = 50)	Retest Subgroup (N = 28) ^a
Exam duration in minutes (mean ± SD)	Mesopic: 8.25 ± 0.45 Red: 9.12 ± 1.03 Cyan: 9.08 ± 1.37	Mesopic: 8.2 ± 0.44 Red: 9.02 ± 0.53 Cyan: 8.56 ± 1.43
95% BCEA in deg ² (median [Q1; Q3])	Mesopic: 10 [6.5; 27.8] Red: 12.1 [4.6; 23] Cyan: 17.7 [6.4; 34.9]	Mesopic: 9.1 [5.8; 23.4] Red: 11.2 [5.2; 16.9] Cyan: 21.8 [7.5; 35.9]
FP rate in false-positive responses/ total number of catch trials (median [Q1; Q3])	Mesopic: 0 [0; 0.13] Red: 0 [0; 0.11] Cyan: 0 [0; 0.11]	Mesopic: 0 [0; 0.13] Red: 0 [0; 0.11] Cyan: 0 [0; 0.1]
Wrong pressure events in wrong pressure events per minute (median [Q1; Q3])	Mesopic: 0.13 [0.1; 0.25] Red: 0.16 [0; 0.26] Cyan: 0.09 [0; 0.19]	Mesopic: 0.15 [0.11; 0.33] Red: 0.12 [0; 0.23] Cyan: 0.04 [0; 0.19]

The rate of false-positive responses (FP rate) was defined as the rate of responses to a suprathreshold stimulus presented to the patient’s blind spot (i.e., Heijl-Krakau method). The rate of wrong pressure events (WPE rate) was defined as the number pressure events outside of the response window of the S-MAIA divided by the examination time. The 95% bivariate contour ellipse area (BCEA) encompassing 95% of the fixation points was evaluated as measure of fixation stability.

^a Please note, the values are derived from the first test run only for comparability to the data of the overall cohort.

Table 3. Cumulative Test-Retest Differences

Test-Retest Difference	Mesopic	Dark-Adapted Cyan	Dark-Adapted Red	Cyan-Red Sensitivity Difference
± 0 dB	43.1%	47.6%	32.3%	31.3%
≤ 2 dB	73.9%	79.2%	75.1%	68.3%
≤ 4 dB	90.3%	90.2%	90.3%	84.6%
≤ 6 dB	96.0%	95.3%	95.6%	92.2%

Influence of Patient-Specific (“Global”) Factors on Retest Reliability

To investigate to what degree retest reliability between patients may be explained by patient-specific (“global”) factors, such as age, mean sensitivity, and “patient reliability indices” as shown in Table 2 (i.e., false-positive responses, wrong pressure events, and fixation stability), we evaluated the variance between patients in retest variability that was explained by these factors using the R^2 for multiple linear

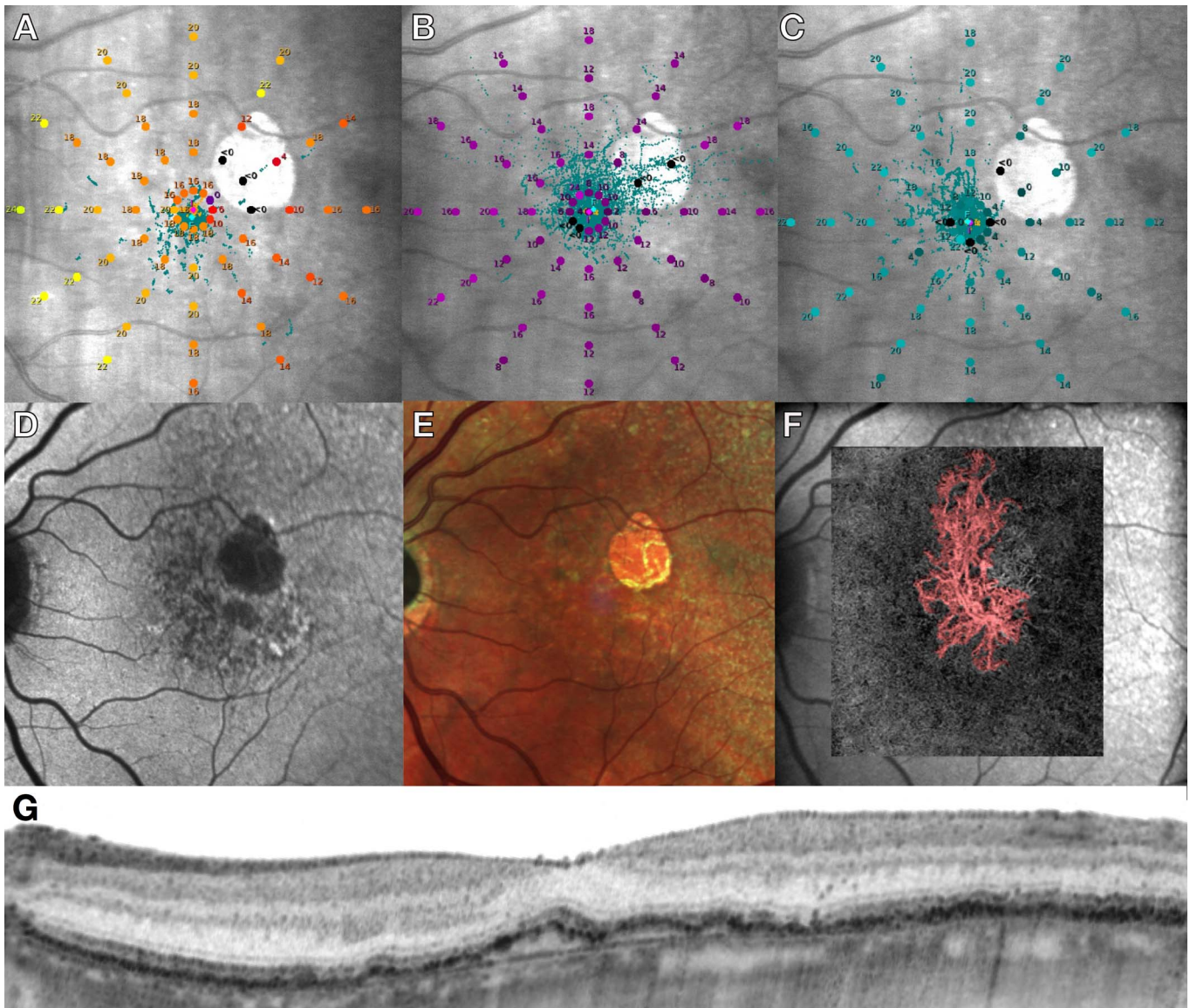


Figure 1. Perimetry grid and multimodal imaging. The Figure shows the left eye of a 74-year-old female patient with treatment-naïve qCNV secondary to AMD as well as atrophy of the retinal pigment epithelium. The mesopic (A), dark-adapted red (B), and dark-adapted cyan (C) test grid consisted of 61 stimuli covering the central 18° of the retina. The test points were evenly spread in five rings at 1°, 3°, 5°, and 9° around a central test-point. FAF (30° × 30°, [D]), multicolor imaging (30° × 30°, [E]), swept-source OCT-A (F) and SD-OCT (G) imaging were part of the multimodal imaging protocol.

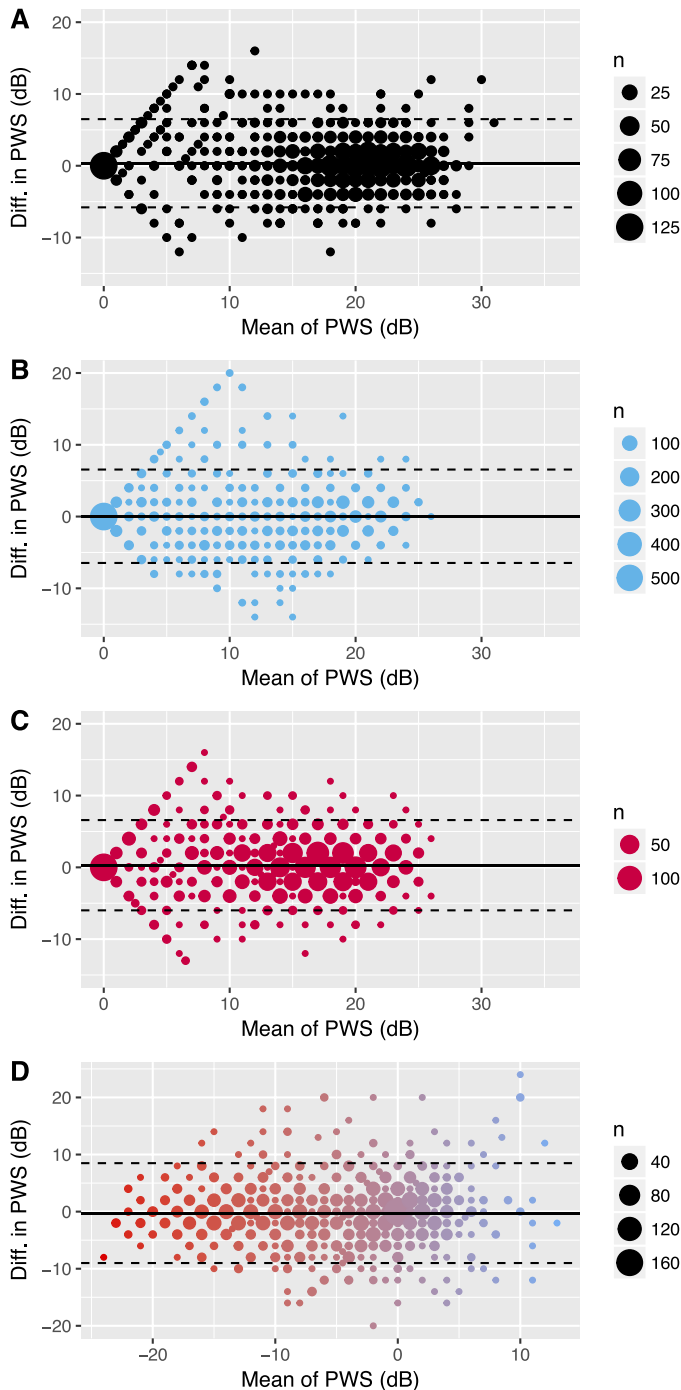


Figure 2. Bland-Altman plots. Bland-Altman plots for mesopic (A), dark-adapted cyan (B), dark-adapted red (C) testing, and the cyan–red difference (D). The x-axis shows the mean pointwise sensitivity (PWS). The PWS difference between the two tests (first minus second test) is indicated on the y-axis. The overall mean difference is illustrated by the *solid line*; the 95% limits of agreement are marked by the two *dashed lines*. The size of individual *circles* illustrates the count of overlapping data points. For all three types of testing no convergence is observable towards the upper end of the dynamic range, indicating that no (relevant) ceiling effect was observable. However, significant convergence

regressions. The mean sensitivity, wrong pressure event rate, false-positive response rate, fixation stability, exam duration, average reaction time, and patient age only explained 55.0% (mesopic), 54.2% (DA cyan), and 64.2% (DA red) of the between-patient variance in retest variability as shown in [Table 4](#). Notably, for all three types of testing, the rate of wrong pressure events provided more information with regard to retest variability than the rate of false-positive responses. For mesopic testing and dark-adapted red testing, higher mean sensitivity, stable fixation (represented by the 95% contour ellipse area), and high BCVA were associated with lower retest variability. For dark-adapted cyan testing, the rate of wrong pressure events was the most important predictor of increased retest variability ([Table 4](#)).

Influence of Test Point–Specific (“Local”) Factors on Retest Reliability

In addition, we analyzed localized factors influencing the retest reliability. For mesopic testing, a mixed model analysis revealed that a location-specific loss of sensitivity was associated with an increase in pointwise retest variability ([effect estimate] $-0.18 \pm 0.05 \text{ dB}^2/\text{dB}$ of sensitivity deviation, $P < 0.001$ [P values obtained using a likelihood ratio test]). In contrast, eccentricity exhibited no significant effect on retest variability for mesopic testing (as well as the other types of testing). Similarly, for dark-adapted cyan testing, only the location-specific loss of sensitivity had a significant effect on retest variability ($P < 0.001$). However, for dark-adapted cyan testing, sensitivity loss was associated with decreased retest variability ($+0.26 \pm 0.06 \text{ dB}^2/\text{dB}$ of sensitivity deviation). The results for dark-adapted red testing mirrored those for mesopic testing. A decrease in sensitivity was associated with an increase in retest variability ($-0.17 \pm 0.05 \text{ dB}^2/\text{dB}$ of sensitivity deviation).

Cone and Rod Function in Relation to CNV Activity

The influence on sensitivity for the subtypes of CNV activity was assessed. All subtypes of CNV lesions had a lower sensitivity compared to controls. Eyes with qCNV exhibited the lowest reduction of mesopic sensitivity with a mean sensitivity loss of

← towards the lower end of the dynamic range was observable, highlighting the floor effect due to the limited dynamic range of the device.

Table 4. Retest Variability Explained by Patient Reliability Indices

Type	Variance in Retest Variability Explained by Full Model (R^2 [in%])	R^2 (in%) Contribution Averaged Over Orderings Among Regressors							
		Mean sensitivity	log10(BCEA)	BCVA	WPE rate	FP rate	Exam duration	Average reaction time	Age
Mesopic	54.97	15.44	21.20	8.24	2.79	1.58	2.68	2.81	0.23
Dark-adapted cyan	54.19	8.93	1.60	2.08	22.05	5.94	11.74	1.14	0.70
Dark-adapted red	64.18	4.60	25.25	13.48	8.46	0.97	7.11	3.73	0.58

The coefficient-of-determination (R^2) was used to assess the between-subject variance in retest variability explained by “patient reliability indices” through multiple linear regression. The R^2 contribution for the individual “patient reliability indices” was determined by averaging over orderings among regressors. The rate of false-positive responses (FP rate) was defined as the rate of responses to a suprathreshold stimulus presented to the patient’s blind spot (i.e., Heijl-Krakau method). The rate of wrong pressure events (WPE rate) was defined as the number pressure events outside of the response window of the S-MAIA divided by the examination time. The 95% bivariate contour ellipse area (BCEA) encompassing 95% of the fixation points was evaluated as measure of fixation stability.

(mean \pm SD) -2.41 ± 2.87 dB. A greater reduction was seen in eyes with sCNV, demonstrating a mean sensitivity loss of -7.61 ± 5.96 dB, and in eyes with aCNV, showing a mean sensitivity loss of -5.90 ± 4.59 dB (Fig. 3A). Similarly, eyes with qCNV exhibited the least degree of sensitivity loss for dark-adapted cyan and dark-adapted red testing. However, these differences in dependence of CNV subtype were not statistically significant. For all three CNV subtypes, the degree of dark-adapted cyan sensitivity loss significantly exceeded the degree of dark-adapted red (and mesopic) sensitivity loss (cyan-red sensitivity differences [mean \pm SD] -2.63 ± 3.87 dB, $P < 0.001$), indicating that rod dysfunction exceeded cone dysfunction in these eyes.

The additional information provided by dark-adapted two-color FCP was visualized by plotting dark-adapted cyan sensitivity loss against BCVA (Fig. 3B). Especially for eyes with good BCVA, dark-adapted cyan FCP allowed more granular functional assessment, revealing that a subgroup of these eyes exhibited significant dark-adapted cyan dysfunction.

Four exemplary patients exhibiting normative versus decreased BCVA and/or moderate versus severe dark-adapted cyan dysfunction are labeled in Figure 3B and visualized in Figure 5. Lastly, analysis of pointwise sensitivity revealed a strong linear correlation of mesopic with dark-adapted red sensitivity loss ($R^2 = 0.718$, Fig. 4). In contrast, the relationship between dark-adapted cyan sensitivity

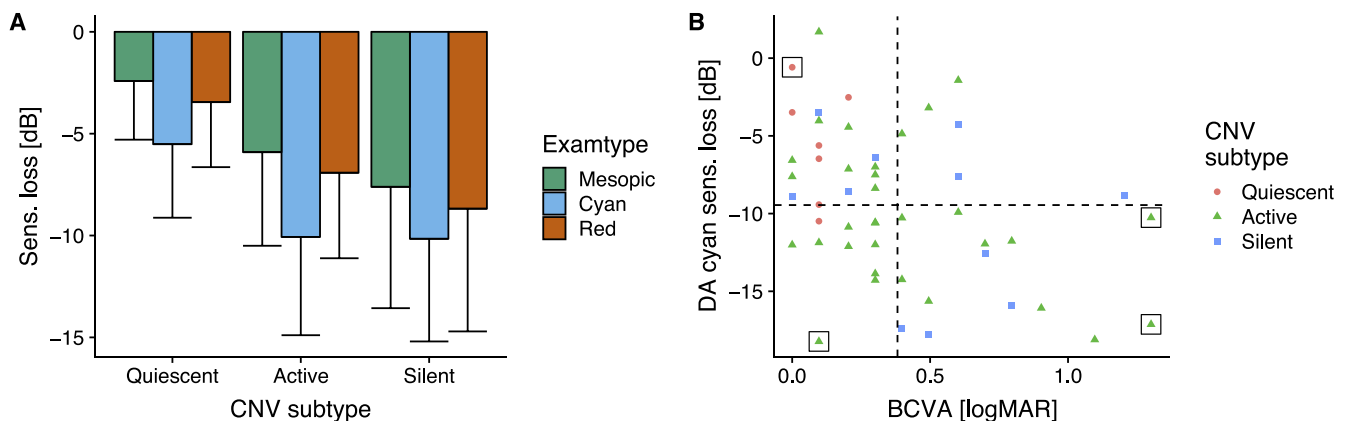


Figure 3. Sensitivity loss in dependence of CNV subtype. The bar graph in (A; bar indicates mean, error bar indicates SD) shows the overall sensitivity loss for the 50 eyes in dependence of the CNV subtype. The dot plot in (B) shows the overall DA cyan sensitivity loss in dependence of the BCVA. The dashed lines indicate the mean DA cyan sensitivity loss (horizontal line) and mean BCVA (vertical line). Notably, the degree of DA cyan sensitivity loss may be highly variable for eyes with good visual acuity highlighting the additional information provided by fundus-controlled perimetry. The four eyes shown in Figure 5 were labeled with black boxes.

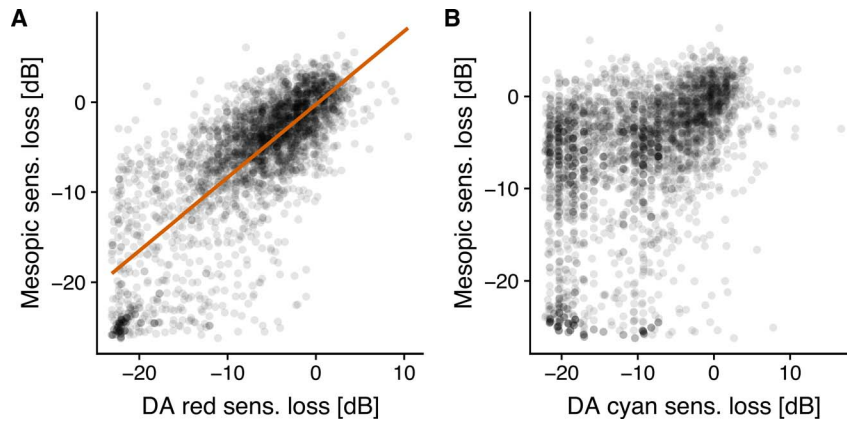


Figure 4. Rod and cone dysfunction. Analysis of pointwise sensitivity revealed a strong linear correlation of mesopic with DA red sensitivity loss (A). In contrast, the relationship between DA cyan sensitivity loss with mesopic sensitivity loss was nonlinear (B). Isolated DA cyan sensitivity loss was observed without mesopic sensitivity loss. However, all test points with some degree of mesopic sensitivity loss exhibited also DA cyan sensitivity loss.

loss with mesopic sensitivity loss was nonlinear. Isolated dark-adapted cyan sensitivity loss was observed without concurrent mesopic sensitivity loss. However, all test points with some degree of mesopic sensitivity loss exhibited (always) concurrent dark-adapted cyan sensitivity loss.

Discussion

Our results indicate that the S-MAIA device allows for reliable topographic testing of mesopic, dark-adapted cyan and red sensitivity in patients with CNV secondary to AMD. Three subgroups of patients with CNV secondary to AMD were included (treatment-naïve qCNV, aCNV, and sCNV), demonstrating that even in eyes currently maintaining a high BCVA, mesopic and dark-adapted two-color FCP already allows for detection of retinal dysfunction. Further, the results resemble previous reports from non-neovascular AMD that impairment of rod function exceeds cone dysfunction.^{16,27–29} Hereby, FCP may compensate for specific drawbacks of BCVA, including the ceiling effect and very limited spatial resolution (i.e., information limited to the fovea or preferred retinal locus). Based on our findings, mesopic and two-color dark-adapted FCP appears to be a suitable complementing outcome measure in clinical trials in CNV secondary to AMD as outlined in the following.

Retest Reliability and Dynamic Range

While previous studies have investigated the applicability of mesopic FCP in CNV secondary to

AMD,^{11–14,30–40} precise information on the retest reliability has been lacking. Hartmann et al.¹⁴ observed a concordance correlation coefficient of 0.85 suggesting overall good agreement. However, the pointwise CoR is not provided in their study. In our cohort, the pointwise CoR as indicator of retest reliability was 5.99 dB for mesopic, 6.14 dB for dark-adapted cyan, and 6.06 dB for dark-adapted red testing indicating good retest reliability. For the mean sensitivity, the retest reliability was naturally even better with values of 1.31 dB for mesopic, 1.19 dB for dark-adapted cyan, and 0.89 dB for dark-adapted red testing. More importantly, the retest variability was mostly homoscedastic across the dynamic range and exhibited no ceiling effects for all three types of testing in the Bland-Altman plots (Fig. 2). This means, that FCP – in contrast with BCVA⁸ – would perform especially well for patients with good pretreatment retinal function and allow for clinical trial designs including eyes with early lesions. Floor effects were observable towards to the lower end of the dynamic range for all three types of testing. While the dynamic range was significantly larger for dark-adapted testing (now 36 dB) as compared to previous version of the device,¹⁹ positive treatment-effects as well as deterioration of sensitivity at test points with a very low pretreatment sensitivity (i.e., <5 dB) may be underestimated. This again highlights that CNV lesions with mild-to-moderate structural and functional alterations may be more suitable to investigate the benefit of additive therapeutic strategies with the S-MAIA than CNV lesions with severe degenerative alterations of the retina (i.e., mean sensitivity <5 dB).

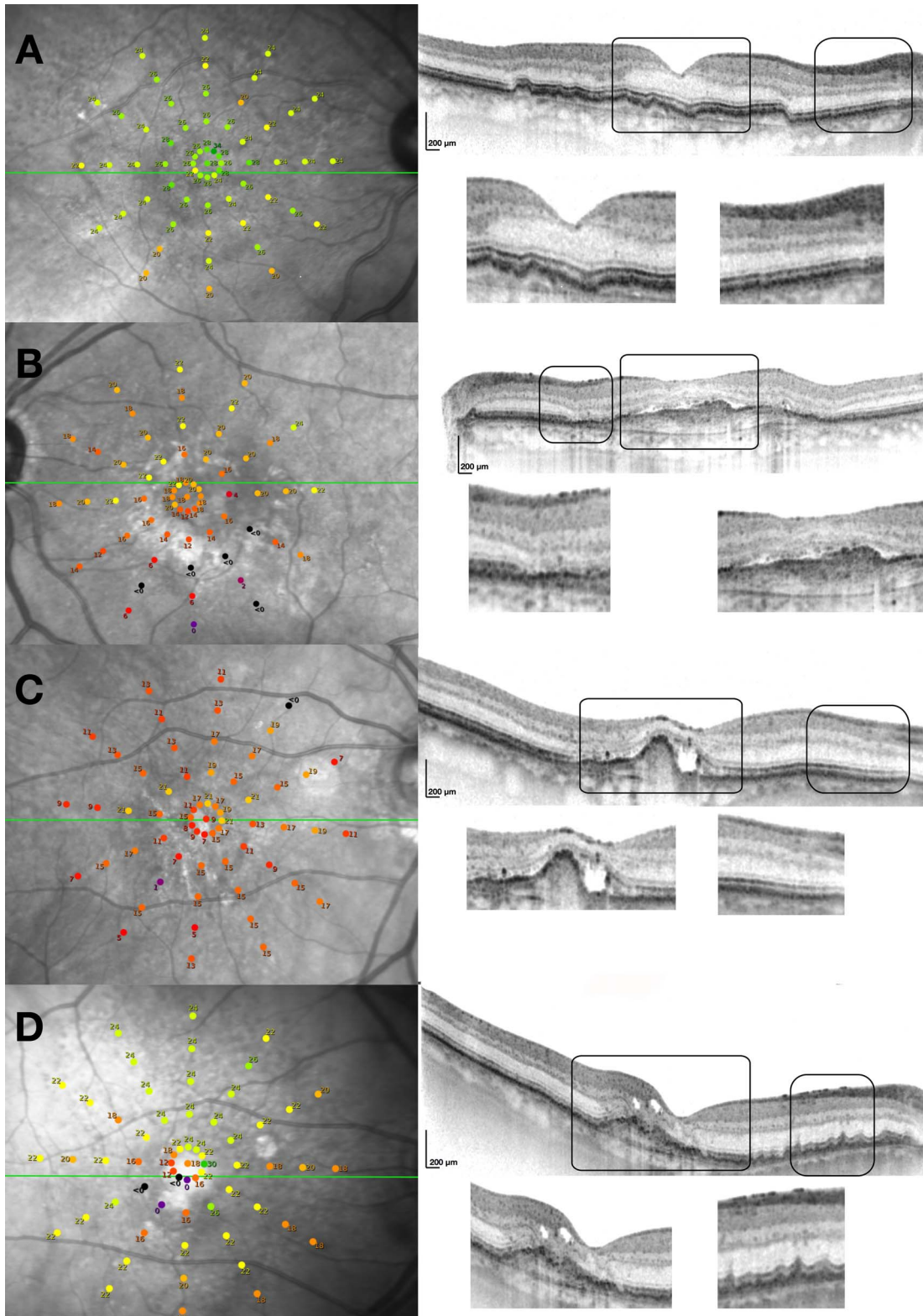


Figure 5. Exemplary patients. (A) Shows the right eye of a 78-year-old female patient with treatment-naïve qCNV. This patient is also marked in [Figure 3B](#) by the *upper left box* displaying a mean sensitivity loss of -0.59 dB in dark-adapted cyan testing and a BCVA of 0.0 logMAR. The outer retinal hyperreflective bands 1-4 are entirely intact despite the presence of a qCNV seen as flat fibrovascular retinal pigment epithelial detachment (PED, “double-layer sign”). (B) Depicts the right eye of a 70-year-old patient classified as aCNV. The

→

← patient (lower left box in Figure 3B) shows a sensitivity of -18.23 dB for dark-adapted cyan testing with almost normative BCVA of 0.1 logMAR. Hereby, the subretinal fluid appears to severely affect rod function, which is dependent on the retinal pigment epithelium (canonical visual cycle). In contrast, the cone-dependent BCVA is largely unaffected, which may be explained by the cone-specific visual cycle, which is independent of the pigment epithelium. ([C], upper right box in Figure 3B, 89-year-old female patient) and ([D], lower right box in Figure 3B, 70-year-old male patient) show both patients with a severely reduced BCVA of 1.3 logMAR. Both patients exhibit centrally distinct alterations of the outer retinal hyperreflective bands. The patient in (C) shows relatively normal outer retinal anatomy outside of the lesion and accordingly exhibits a moderate dark-adapted cyan sensitivity loss of -10.26 dB. In contrast, the patient in (D) exhibits a marked dark-adapted cyan sensitivity loss -17.3 dB in line with the marked reticular pseudodrusen (subretinal drusenoid deposits).

Applicability of “Patient Reliability Indices”

Multiple criteria have been proposed and used to select patients with good retest reliability for clinical studies. Prominently, the rate of false-positive responses to suprathreshold stimuli to the optic nerve head (i.e., Heijl-Krakau method) has been used previously as an exclusion criterion (e.g., with a cutoff of $>25\%$ or $>33\%$).^{41,42} In our data, the rate of false-positive responses was not a very accurate predictor of retest reliability, while at the same time increasing the examination time. Wrong pressure events, however, (pressure events outside of the response window of the S-MAIA), which do not increase the examination time, were more informative with regard to retest variability. In conjunction with previous glaucoma studies, this suggested that wrong pressure events could eliminate the necessity of (time-consuming) false-positive catch-trials in future studies.²¹ Interestingly, the wrong pressure events had the most significant association with dark-adapted cyan retest variability, which may be explained by the slightly longer examination times and lower dark-adapted cyan mean sensitivity; that is, the patient-specific rate of wrong pressure events has more chance to affect the test results in consideration of the relatively prolonged staircase procedure. The 95% bivariate contour ellipse area (as measure of fixation stability) was an important predictor of the retest variability for mesopic and dark-adapted red (both reflecting predominantly cone function), but not for dark-adapted cyan testing (reflecting predominantly rod function). In conjunction, this suggests that fixation stability is highly associated with cone function and, thus, to the retest variability of the respective tests. The alternative hypothesis, that the increased retest variability in eyes with unstable fixation is due to insufficient fundus tracking by the device, appears unlikely, since this relationship was not observed for dark-adapted cyan testing. Given the limited variance in retest variability explained by individual “patient reliability indices,” duplicate

testing with determination of the actual retest reliability or an inclusion rule that takes into consideration all of the “patient reliability indices” appears to be a more prudent approach than relying solely on false-positive responses.

Cone and Rod Function in CNV Secondary to AMD

Previous histopathologic and psychophysical studies have pointed towards increased vulnerability of rod photoreceptors in age-related macular disease.^{28,43–45} Herein, for all three subtypes of CNV activity, dark-adapted cyan sensitivity losses exceeded dark-adapted red sensitivity loss (and mesopic sensitivity loss) in accordance with the current understanding of the impact of AMD on photoreceptor subtypes. Yet, to the best of our knowledge this is the first study to describe specifically the degree of macular rod dysfunction in the setting of CNV secondary to AMD. Moreover, dark-adapted cyan sensitivity loss was observed in a significant proportion of test points in absence of mesopic sensitivity loss (Fig. 4A), while mesopic sensitivity loss appeared always to be associated with dark-adapted cyan sensitivity loss (Fig. 4B). This nonlinear relationship could indicate that rod dysfunction not only exceeds, but also temporally precedes cone dysfunction in CNV secondary to AMD. A longitudinal study will be necessary to confirm this finding.

Limitations

With regard to applicability in clinical trials, the intervisit retest reliability as well as the natural history of progression of dysfunction (especially in eyes with treatment-naïve qCNV) will need to be addressed in a longitudinal study. Furthermore, dark adaptometry studies suggest that the final rod-plateau may be reached even later than 30 minutes in a subset of patients with AMD. Therefore, the effect of differential dark adaptation periods on dark-adapted FCP will need to be addressed.⁴⁶ Lastly, we used a polar

testing grid with uneven spacing between the test points. Our estimates for the mean sensitivity losses, therefore, represent spatially-weighted indices with more weight given towards the central retina.²⁰

In summary, our study demonstrated that mesopic and dark-adapted two-color FCP allows for precise assessment of retinal sensitivity in patients with neovascular AMD. We provided estimates for the retest reliability to define significant changes in visual function at individual retinal loci over time. Further, we investigated the predictive value of “patient-reliability indices” to inform data-driven eligibility/exclusion criteria for clinical trials. In terms of retinal function, our data indicated that rod dysfunction exceeds cone dysfunction in eyes with CNV secondary to AMD and suggested that potentially rod dysfunction also temporally precedes cone dysfunction. In conjunction, this constitutes the basis for a potential application of mesopic and dark-adapted FCP as a novel functional outcome measure in interventional clinical trials in nAMD.

Acknowledgments

Supported by the ProRETINA Foundation [Doctoral Research Support Grant to Lvde], Novartis Pharma GmbH [EYEnovative Förderpreis 2017 to MP], BONFOR Program of the Faculty of Medicine, University of Bonn [Grant No O-137.0022 and O-137.0025 to MP] and by the German Research Foundation (DFG) [FL658/4-1 and FL658/4-2 to MF]. CenterVue SpA, Padova, Italy has provided research material (S-MAIA) for the conduct of this study. CenterVue had no role in the design or conduct of the experiments.

Disclosure: **L. von der Emde**, Heidelberg Engineering (F), Optos (F), Zeiss (F), CenterVue (F); **M. Pfau**, Heidelberg Engineering (F), Optos (F), Zeiss (F), CenterVue (F); **S. Thiele**, Heidelberg Engineering (F), Optos (F), Zeiss (F), CenterVue (F); **P.T. Möller**, Heidelberg Engineering (F), Optos (F), Zeiss (F), CenterVue (F); **R. Hassenrik**, Heidelberg Engineering (F), Optos (F), Zeiss (F), CenterVue (F); **M. Fleckenstein**, Heidelberg engineering (F,R) Optos (F), Zeiss (F), CenterVue (F); **F.G. Holz**, Heidelberg Engineering (C,F,R), Optos (CF), Zeiss (C,F), CenterVue (F); **S. Schmitz-Valckenberg**, Heidelberg Engineering (F,R), Optos (F), Zeiss (F, R), CenterVue (F)

References

1. Lim LS, Mitchell P, Seddon JM, Holz FG, Wong TY. Age-related macular degeneration. *Lancet*. 2012;379:1728–1738.
2. Miller JW. Beyond VEGF-The Weisenfeld Lecture. *Invest Ophthalmol Vis Sci*. 2016;57:6911–6918.
3. Holz FG, Tadayoni R, Beatty S, et al. Multi-country real-life experience of anti-vascular endothelial growth factor therapy for wet age-related macular degeneration. *Br J Ophthalmol*. 2015;99:220–226.
4. Rofagha S, Bhisitkul RB, Boyer DS, Sadda SR, Zhang K. Seven-year outcomes in ranibizumab-treated patients in ANCHOR, MARINA, and HORIZON: a multicenter cohort study (SEVEN-UP). *Ophthalmology*. 2013;120:2292–2299.
5. Heier JS, Brown DM, Chong V, et al. Intravitreal aflibercept (VEGF trap-eye) in wet age-related macular degeneration. *Ophthalmology*. 2012;119:2537–2548.
6. Heier JS, Antoszyk AN, Pavan PR, et al. Ranibizumab for treatment of neovascular age-related macular degeneration: a phase I/II multicenter, controlled, multidose study. *Ophthalmology*. 2006;113:633.e1–e4.
7. Rosenfeld PJ, Brown DM, Heier JS, et al. Ranibizumab for neovascular age-related macular degeneration. *N Engl J Med*. 2006;355:1419–1431.
8. Amoaku WM, Chakravarthy U, Gale R, et al. Defining response to anti-VEGF therapies in neovascular AMD. *Eye (Lond)*. 2015;29:721–731.
9. Vujosevic S, Pucci P, Casciano M, et al. Long-term longitudinal modifications in mesopic microperimetry in early and intermediate age-related macular degeneration. *Graefes Arch Clin Exp Ophthalmol*. 2017;255:301–309.
10. Wu Z, Ayton LN, Luu CD, Guymer RH. Longitudinal changes in microperimetry and low luminance visual acuity in age-related macular degeneration. *JAMA Ophthalmol*. 2015;133:442–448.
11. Sulzbacher F, Roberts P, Munk MR, et al. Relationship of retinal morphology and retinal sensitivity in the treatment of neovascular age-related macular degeneration using aflibercept. *Invest Ophthalmol Vis Sci*. 2014;56:1158–1167.
12. Sabour-Pickett S, Loughman J, Nolan JM, et al. Visual performance in patients with neovascular age-related macular degeneration undergoing

- treatment with intravitreal ranibizumab. *J Ophthalmol.* 2013;2013:268438.
13. Hautamaki A, Oikkonen J, Onkamo P, Immonen I. Correlation between components of newly diagnosed exudative age-related macular degeneration lesion and focal retinal sensitivity. *Acta Ophthalmol.* 2014;92:51–58.
 14. Hartmann KI, Oster SF, Amini P, Bartsch D-U, Cheng L, Freeman WR. SLO-Microperimetry in Wet Age-Related Macular Degeneration During Anti-VEGF Therapy. *Ophthalm Surg Lasers Imaging Retina.* 2015;46:824–830.
 15. Curcio CA, Millican CL, Allen KA, Kalina RE. Aging of the Human Photoreceptor Mosaic: Evidence for Selective Vulnerability of Rods in Central Retina. *Invest Ophthalmol Vis Sci.* 1993;34:3278–3296.
 16. Pfau M, Lindner M, Gliem M, et al. Mesopic and dark-adapted two-color fundus-controlled perimetry in patients with cuticular, reticular, and soft drusen [published online August 1, 2018]. *Eye (Lond)*. <https://doi.org/10.1038/s41433-018-0183-3>
 17. Pfau M, Muller PL, von der Emde L, et al. Mesopic and dark-adapted two-color fundus-controlled perimetry in geographic atrophy secondary to age-related macular degeneration [published online October 8, 2018]. *Retina*. <https://doi.org/10.1097/IAE.0000000000002337>
 18. Pfau M, Lindner M, Fleckenstein M, et al. Test-Retest reliability of scotopic and mesopic fundus-controlled perimetry using a modified MAIA (macular integrity assessment) in normal eyes. *Ophthalmologica.* 2017;237:42–54.
 19. Pfau M, Lindner M, Muller PL, et al. Effective dynamic range and retest reliability of dark-adapted two-color fundus-controlled perimetry in patients with macular diseases. *Invest Ophthalmol Vis Sci.* 2017;58: BIO158–BIO167.
 20. Pfau M, Lindner M, Steinberg JS, et al. Visual field indices and patterns of visual field deficits in mesopic and dark-adapted two-colour fundus-controlled perimetry in macular diseases. *Br J Ophthalmol.* 2018;102:1054–1059.
 21. Olsson J, Bengtsson B, Heijl A, Rootzen H. An improved method to estimate frequency of false positive answers in computerized perimetry. *Acta Ophthalmol Scand.* 1997;75:181–183.
 22. Querques G, Srour M, Massamba N, et al. Functional characterization and multimodal imaging of treatment-naive “quiescent” choroidal neovascularization. *Invest Ophthalmol Vis Sci.* 2013;54:6886–6892.
 23. Carnevali A, Cicinelli MV, Capuano V, et al. Optical coherence tomography angiography: a useful tool for diagnosis of treatment-naive quiescent choroidal neovascularization. *Am J Ophthalmol.* 2016;169:189–198.
 24. Roisman L, Zhang Q, Wang RK, et al. Optical coherence tomography angiography of asymptomatic neovascularization in intermediate age-related macular degeneration. *Ophthalmology.* 2016;123:1309–1319.
 25. Steinman RM. Effect of target size, luminance, and color on monocular fixation. *J Opt Soc Am.* 1965;55:1158–1164.
 26. Bland JM, Altman DG. Statistical methods for assessing agreement between two methods of clinical measurement. *Lancet.* 1986;1:307–310.
 27. Curcio CA, Medeiros NE, Millican CL. Photoreceptor loss in age-related macular degeneration. *Invest Ophthalmol Vis Sci.* 1996;37:1236–1249.
 28. Owsley C, Jackson GR, Cideciyan A V., et al. Psychophysical evidence for rod vulnerability in age-related macular degeneration. *Invest Ophthalmol Vis Sci.* 2000;41:267–273.
 29. Steinberg JS, Fitzke FW, Fimmers R, Fleckenstein M, Holz FG, Schmitz-Valckenberg S. Scotopic and photopic microperimetry in patients with reticular drusen and age-related macular degeneration. *JAMA Ophthalmol.* 2015;133:690–697.
 30. Ergun E, Maar N, Radner W, Barbazetto I, Schmidt-Erfurth U, Stur M. Scotoma size and reading speed in patients with subfoveal occult choroidal neovascularization in age-related macular degeneration. *Ophthalmology.* 2003;110:65–69.
 31. Munk MR, Kiss C, Huf W, et al. One year follow-up of functional recovery in neovascular AMD during monthly anti-VEGF treatment. *Am J Ophthalmol.* 2013;156:633–643.
 32. Ozdemir H, Karacorlu M, Senturk F, Karacorlu SA, Uysal O. Microperimetric changes after intravitreal bevacizumab injection for exudative age-related macular degeneration. *Acta Ophthalmol.* 2012;90:71–75.
 33. Sulzbacher F, Kiss C, Kaider A, et al. Correlation of OCT characteristics and retinal sensitivity in neovascular age-related macular degeneration in the course of monthly ranibizumab treatment. *Invest Ophthalmol Vis Sci.* 2013;54:1310–1315.
 34. Alexander P, Mushtaq F, Osmond C, Amoaku W. Microperimetric changes in neovascular age-related macular degeneration treated with ranibizumab. *Eye (Lond)*. 2012;26:678–683.
 35. Dunavoelgyi R, Sacu S, Simader C, Pruenste C, Schmidt-Erfurth U. Changes in macular sensitivity after reduced fluence photodynamic therapy

- combined with intravitreal triamcinolone. *Acta Ophthalmol.* 2011;89:166–171.
36. Fujii GY, De Juan EJ, Humayun MS, Sunness JS, Chang TS, Rossi J V. Characteristics of visual loss by scanning laser ophthalmoscope microperimetry in eyes with subfoveal choroidal neovascularization secondary to age-related macular degeneration. *Am J Ophthalmol.* 2003;136:1067–1078.
 37. Grenga PL, Fragiotta S, Meduri A, Lupo S, Marengo M, Vingolo EM. Fixation stability measurements in patients with neovascular age-related macular degeneration treated with ranibizumab. *Can J Ophthalmol.* 2013;48:394–399.
 38. Mettu PS, Sarin N, Stinnett SS, Toth CA. Recovery of the neurosensory retina after macular translocation surgery is independent of preoperative macular sensitivity in neovascular age-related macular degeneration. *Retina.* 2011;31:1637–1649.
 39. Chieh JJ, Stinnett SS, Toth CA. Central and pericentral retinal sensitivity after macular translocation surgery. *Retina.* 2008;28:1522–1529.
 40. Cho HJ, Kim CG, Yoo SJ, et al. Retinal functional changes measured by microperimetry in neovascular age-related macular degeneration treated with ranibizumab. *Am J Ophthalmol.* 2013;155:118–126.e1.
 41. Wu Z, Ayton LN, Guymer RH, Luu CD. Intrasection test – retest variability of microperimetry in age-related macular degeneration. *Assoc Res Vis Ophthalmol.* 2013;54:7378–7385.
 42. Yamamoto S, Sugawara T, Murakami A, et al. Topical isopropyl unoprostone for retinitis pigmentosa: microperimetric results of the phase 2 clinical study. *Ophthalmol Ther.* 2012;1:5.
 43. Curcio CA, Allen KA. Aging of the human photoreceptor mosaic: evidence for selective vulnerability of rods in central retina. *Invest Ophthalmol Vis Sci.* 1993;34:3278–3296.
 44. Jackson GR, Owsley C, Curcio CA. Photoreceptor degeneration and dysfunction in aging and age-related maculopathy. *Ageing Res Rev.* 2002;1:381–396.
 45. Owsley C, McGwin G, Clark ME, et al. Delayed rod-mediated dark adaptation is a functional biomarker for incident early age-related macular degeneration. *Ophthalmology.* 2016;123:344–351.
 46. Jackson GR, Scott IU, Kim IK, Quillen DA, Iannaccone A, Edwards JG. Diagnostic sensitivity and specificity of dark adaptometry for detection of age-related macular degeneration. *Invest Ophthalmol Vis Sci.* 2014;55:1427–1431.